ESI Preprints **Not Peer-reviewed**

Identifying Areas of High Gold Potential Using Geochemical Prospecting Methods: The Tenado area in the Boromo Birimian Belt, West-Central Burkina Faso, West Africa

Fayçal Tarnagda
Laboratoire Géosciences et Environnement (LaGe), département des Sciences de la Terre, Ouagadougou, Burkina Faso
Université Joseph KI Zerbo (UJKZ), Ouagadougou. Burkina Faso
Pascal Ouiya
Laboratoire Géosciences et Environnement (LaGe), département des Sciences de la Terre, Ouagadougou, Burkina Faso
Ecole Normale Supérieure (ENS), Institut Sciences et Technologies (IST), Ouagadougou. Burkina Faso
Sâga Sawadogo
Ecole Normale Supérieure (ENS), Institut Sciences et Technologies (IST), Ouagadougou. Burkina Faso
Université Joseph KI Zerbo (UJKZ), Ouagadougou. Burkina Faso

Doi: 10.19044/esipreprint.12.2023.p599

Approved: 12 December 2023
Posted: 14 December 2023

Cite As:
Tarnagda F., Ouiya P. & Sawadogo S. (2023). *Identifying Areas of High Gold Potential Using Geochemical Prospecting Methods: The Tenado area in the Boromo Birimian Belt, West-Central Burkina Faso, West Africa.*. ESI Preprints.
https://doi.org/10.19044/esipreprint.12.2023.p599

Abstract

The investigation area is located in the central-western region of Burkina Faso, in a geological environment that incorporates the Paleoproterozoic formations of the Boromo greenstone belt. The area already hosts several gold showings and an active zinc mine, but no major gold deposits. The aim of this study is to define target areas with high gold potential for further prospecting. To meet this objective, we used mainly geochemical methods.

The combination of gold content in stream sediments and litho-geochemical data has enabled us to highlight two areas of gold (Au) and various metal

anomalies. Gold content in stream sediments is mainly influenced by that of the source rock from which it is derived. Indeed. high gold anomalies are found in clay sediments more than in sand sediments. Clay sediments are derived from basic rocks (basalt) and intermediate rocks (andesite-dacite). whereas gold-poor sandy sediments are derived from granitoids. Basic to intermediate rocks are fertile for primary gold. Anomaly zone one (01) in the northern part of the study area (Kelsio, Zoula, Poa and Dyoro) and anomaly zone two (02) in the southern part of the study area (Kwademan. Baguiomo, Bérédo, Bonga and Baganapou) show occurrences of mainly gold and various metals (Zn. Cu. Ni).

Keywords: Anomaly area, Paleoproterozoic, Boromo Birimian Belt, Burkina Faso

1. Introduction

Many studies of the West African craton have shown that it is rich in metal mineralization (Milési et al., 1989, 1992; Groves et al., 1998; Markwitz et al., 2016; Goldfarb et al., 2017; Masurel et al., 2021). This craton is made up of two major dorsals. notably the Réguibat ridge to the north and the Man/Leo ridge to the south. In the Man/Leo ridge. Archean formations lie to the east and Paleoproterozoic formations to the west (Fig.1-A). The Paleoproterozoic formations in this western part of the dorsal are still referred to as Birimian formations (Kitson, 1918; Junner, 1940; Bessoles, 1977) and are affected by the Eburnian orogeny (Feybesse et al., 2006). These Birimian formations consist of alternating belts of greenstone cut by different generations of granitoids (Hirdes et al., 1996; Doumbia et al., 1998; Gasquet et al., 2003; Baratoux et al., 2011; Ganne et al., 2014).

Most of the orogenic gold deposits in the Man/Léo dorsal and in Burkina Faso in particular are contained in greenstone belts (Castaing et al., 2003; Giovenazzo et al., 2018); Fig.1-B). In view of the mining potential offered by these Birimian volcano-sedimentary belts. we focused on the Boromo greenstone belt. which is already known for its gold and base metal potential (Fig.1-B). Today, geochemical prospecting is increasingly used in mineral exploration to detect and delineate areas of geochemical anomalies of one or more metals(Carranza. 2010; Yousefi et al.. 2013; Abdolmaleki et al., 2014; Darehshiri et al., 2015; Shine et al., 2022). There are several means of geochemical investigation, the implementation of which depends on the element to be investigated. These include litho-geochemistry, soil geochemistry and stream sediment geochemistry for metals. Although stream sediment geochemistry can be used to search for metal anomalies. this type of sample remains transported, and it is imperative to involve other geochemical prospecting methods such as lalitho-geochemistry. Indeed, the

difficulty in analyzing stream sediment data lies in determining the source from which it originates (Ndome Effoudou-Priso et al., 2014; Sorokina. 2019; Noa Tang et al., 2020). The availability of outcropping rock samples near stream sediment sampling points for litho-geochemical analysis would therefore be a major asset in delineating areas with high gold potential.

This study is carried out in the central-western region of Burkina Faso, which was the subject of a geochemical prospecting study in 1982. This work led to the discovery of the Perkoa Zn-Ag sulphide cluster deposit (Franceschi and Ouédraogo. 1982). Since then. other initiatives have followed (Kabore et al., 1989), but to date no major gold (Au) deposit has been discovered in this area. The aim of this work is to delineate zones of interest with high gold potential in the west-central region in order to guide future prospecting for the discovery of a large gold deposit. To achieve this. we used stream sediment and total rock geochemistry (litho-geochemistry) data. We discuss the origin of gold in stream sediments.

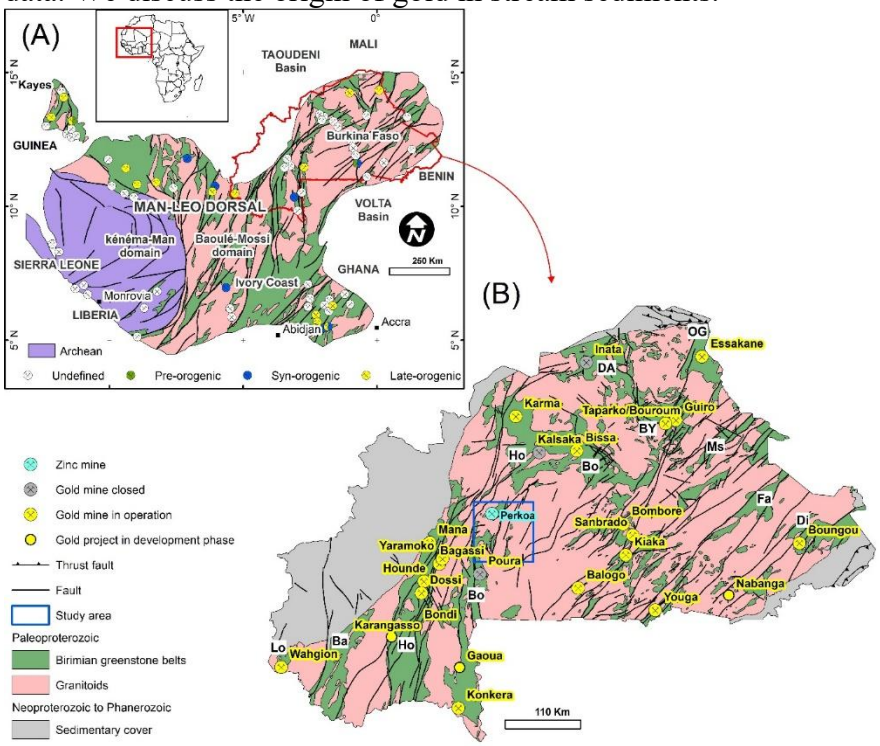

Figure 1. (A) Modified litho-structural and metallogenic map of the Léo Ridge. after Milesi et al.. (2004) and (B) Synthesis geological map of Burkina Faso. modified after Castaing et al.. (2003). LoB: Loumana greenstone belt; BaB: Banfora greenstone belt; Ho: Houndé greenstone belt; BoB: Boromo greenstone belt; MSB: Manga-Sebba greenstone belt; FaB: Fada N'Gourma greenstone belt; DiB: Diapaga greenstone belt; BYB: Yalo greenstone belt; DAB: Djibo-Arbinda greenstone belt; OGB: Oudalan-Gorouol greenstone belt.

2. Regional geological context

The geology of the central-western region is dominated by granitoids and the volcano-sedimentary formations of the Boromo greenstone belt (Fig.2). The combination of granitoids and volcano-sedimentary belt is late cut by dolerite dykes (Castaing et al., 2003; Dahl et al.. 2018). The portion of the Boromo greenstone belt that crosses the study area in the Tenado commune is composed of volcanic rocks. volcano-sedimentary rocks and sedimentary rocks.

The volcanic series is composed of basalt, andesite, dacite and rhyolite. There is also the presence of ultrabasite, most often associated with gabbros (Béziat et al., 2000). The sedimentary formations include metagrites, tuffaceous schists, sericite schists and manganiferous black schists (Schwartz and Melcher, 2003; Chevremont et al., 2003). Intercalations of gabbros, Rhyolites, dolerites and diorites are found throughout the volcano-sedimentary package. These assemblages are organized into greenstone belts by two generations of granitoids in the study area, The first generation is represented by the TTG (Tonalite Trondhjemite Granodiorite) series, which outcrops mainly in the extreme NW and SE of the study area, Their emplacement locally induces amphibolite-facies metamorphism at the contacts with the Boromo greenstone belt formations (Chevremont et al., 2003). The second generation, consisting of biotite granite, porphyritic biotite granite and leucogranite. outcrops throughout the study area (Chevremont et al., 2003 ; Ouedraogo et al., 2003). All these formations are later cut by NW-SE trending dolerite dykes. Structurally. three deformation phases (D1 to D3) are accepted (Feybesse et al.. 1990 ; Baratoux et al., 2011; Metelka et al., 2011). The first phase of deformation (D1) is marked by a general NW-SE shortening and oriented the greenstone belt in a N-S to NE-SW direction. The second deformation phase (D2) is characterized by predominantly sinister shear zones, followed by the final deformation phase (D3). The structures of D3 are of the type : steeply dipping crenulation cleavage. trending E-W on average, and reverse faults dipping shallowly to the north or south. These deformation structures have given rise to a number of hydrothermal deposits in the central west, including the Zn-Ag volcanogenic sulfide cluster (VMS) polymetallic deposit at Perkoa and the Kwademen gold deposit.

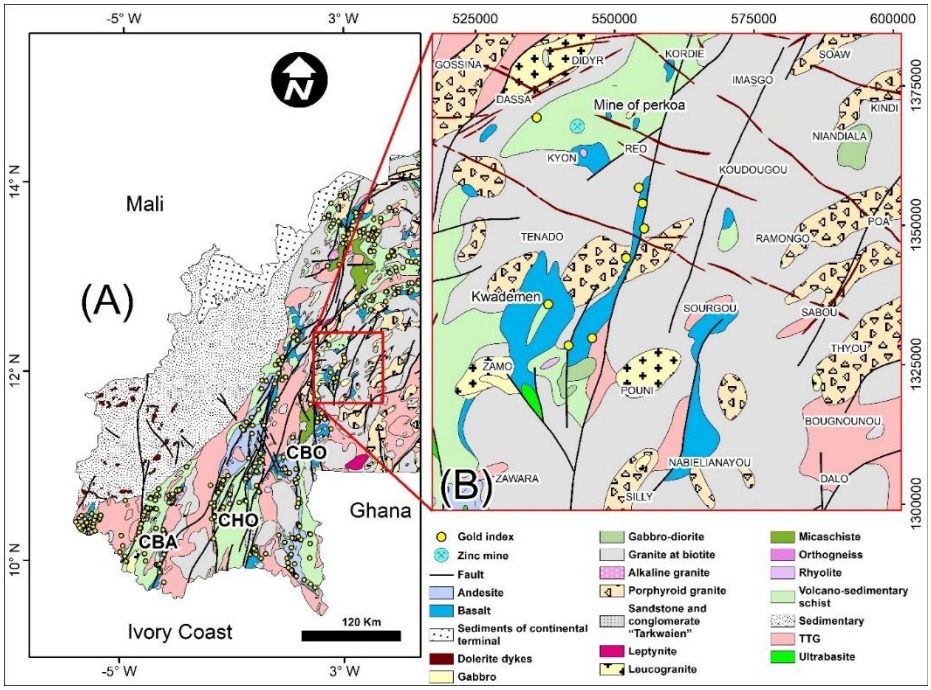

Figure 2. Geological map of the study area. after Castaing et al (2003). (A) Half of geological map; (B) Zoom on study area. (BAB): Banfora greenstone belt; (HOB): Houndé greenstone belt; (BOB): Boromo greenstone belt.

3. Methodology

Total rock geochemistry sampling was carried out on outcrops observed during the mapping phase on a regional scale of 1:200.000. The rocks sampled were conditioned at the BUMIGEB, then underwent treatments ranging from crushing to grinding. The powders obtained by this process are pulverized. sieved to a fine mesh of around 75 microns and then digested with acid (aqua regia) for at least one hour in a graphite heating block. After cooling, the resulting solution was diluted to 12.5 ml with demineralized water, mixed and analyzed by inductively coupled plasma-atomic emission spectrometry (ICP-AES). In all, we acquired 32 results from these analyses, expressed as percentage of oxide weight for major elements and in ppm (parts per million) for trace elements and the various metals analyzed (Au. Ag. Zn. Ni. Cu. etc.).

In addition to these total rock geochemistry data, we also used stream sediment data (284 stream sediment analysis results). These stream sediments were sampled on a regional scale, taking several samples of fine material (1 to 3 kg) deposited in river beds or on banks, The sampling grid is 10 km. i.e. four samples per km2. These samples were sieved at the BUMIGEB laboratory to a mesh size of 63 µm and then sent for ICP AES

analysis at the BRGM laboratory in Orleans, France, The detection limit in these analyses is of the order of 1 ppb.

The geochemical anomaly area delimitation method used in this work is the iso-tenor or iso-contour delimitation method. It was carried out in ArcMap 10.8 mapping software using the geostatistical interpolation method based on the Kriging technique.

4. Results

4.1 Spatial distribution of chemical anomalies

The spatial distribution of gold grades in stream sediment results shows several gold anomaly zones that stand out due to their high concentrations. Most of the high gold grades are isolated and distributed along the banks of the various rivers (Mouhoun, Nazinon and Sissili) drained by their watersheds. with highly variable topography in terms of altitude (240 to 480 m). resulting in significant alluvial input (Fig.3).

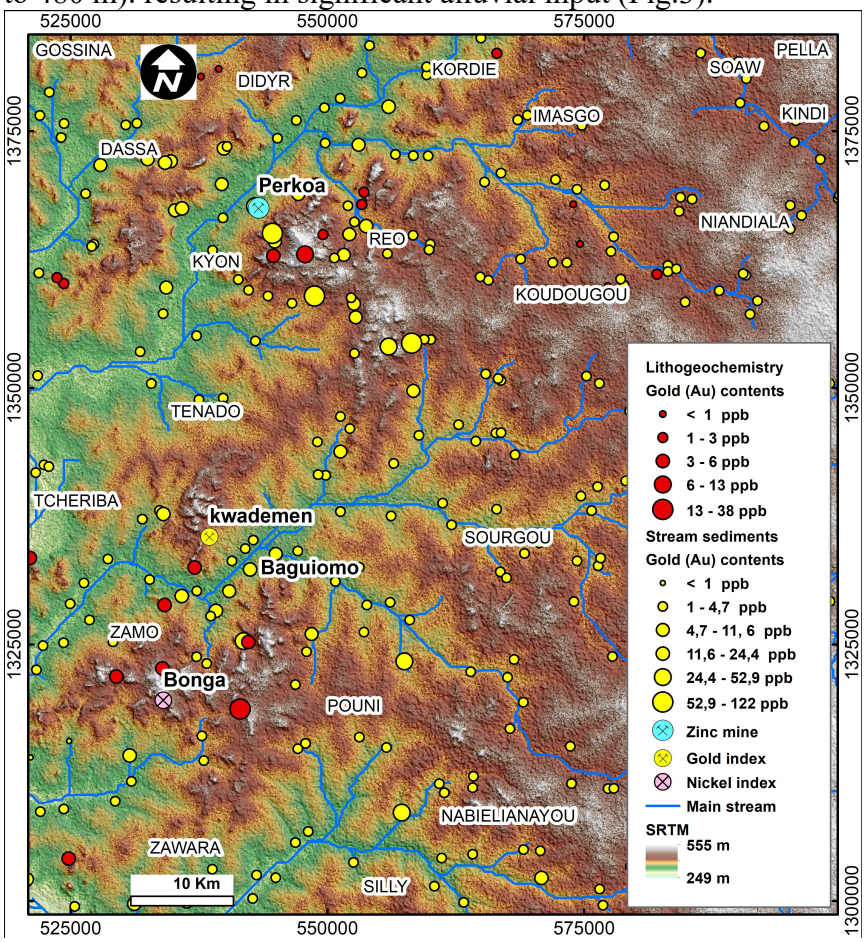

Figure 3. Map showing Au anomalies derived from stream sediment and lithogeochemical data

Analytical data from stream sediments show two (2) major gold (Au) anomaly areas (Fig.4).

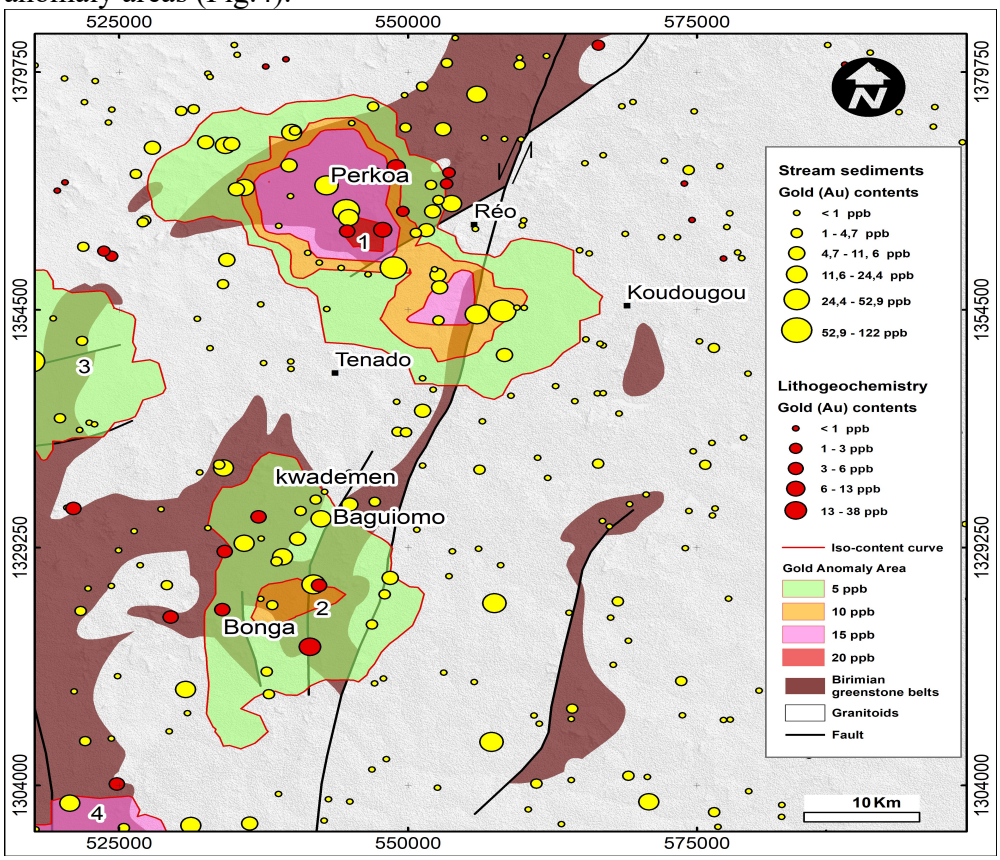

Figure 4. Gold concentration map of stream sediments and in-situ rocks. Two anomalous zones are delineated

The four delineated anomaly areas are mostly located on the Boromo greenstone belt. Within these four zones, two (2) anomaly areas stand out, namely anomaly areas 1 and 2 respectively located around the Perkoa mine and around the Kwademen artisanal mine, due to their high concentrations of certain elements such as A, Zn, Cu and Ni (Table I).

Table I. Anomaly zone 1 and 2 stream sediment data table

Sample	SR399	SR402	OA482	SM406	SR388	SR390	SR387	SR404	OA487	SR400	OA480	SM408	SM410	SM322	SR440	OA489
Anomalie	Zone 1	Zone 1	Zone 1	Zone 1	Zone 1	Zone 1	Zone 1	Zone 1	Zone 1	Zone 1	Zone 1	Zone 1	Zone 1	Zone 1	Zone 1	Zone 1
Material	Argilaux	Argilaux	Argilaux	Argilaux	Argilaux	Argilaux	Argilaux	Argilaux	Argilaux	Argilaux	Argilaux	Argilaux	Argilaux	Argilaux	Argilaux	Argilaux
Long	-2.57	-2.61	-2.59	-2.57	-2.53	-2.55	-2.53	-2.62	-2.68	-2.59	-2.59	-2.63	-2.63	-2.46	-2.70	-2.67
Lat	12.29	12.30	12.35	12.38	12.33	12.29	12.33	12.31	12.37	12.29	12.34	12.42	12.42	12.25	12.41	12.37
SiO_2	45.6	50.4	50.5	52	52.2	57	57.3	57.9	58.2	59.5	59.9	60.3	60.8	61.1	61.8	62
Al_2O_3	24.1	17.5	14.7	17.5	16.1	12.5	17.8	17.1	15.6	13.7	11.9	12.9	13.3	15	13.9	12.8
Fe_2O_3	7.6	9.3	8.2	7.1	8.6	8	6.3	7	5.6	7.2	7.6	6	6.3	7.3	4.5	4.3
CaO		1.1	2.6		1.1					1.1	2.4	1.4	1			
K_2O	1	0.9	0.8	0.7	1.1	0.7	1	1	1	0.9	0.7	0.8	0.8	0.8	1.2	1.1
MnO	0.12	0.29	0.23	0.13	0.17	0.32	0.11	0.11	0.09	0.17	0.15	0.09	0.09	0.11	0.1	0.13
TiO_2	1.27	1.36	1.08	1.23	1.69	2.49	1.43	1.41	1.29	1.39	1.16	1.16	1.3	1.3	1.4	1.42
Co	23	59	48	38	36	49	24	29	18	37	34	25	27	30	20	20
Ni	55	87	70	83	79	63	54	76	35	55	56	76	112	46	37	34
Cu	56	86	76	88	83	60	58	60	29	63	81	41	40	57	24	31
Au	1	1	9	6	4.5	71.4	8.3	1	9.3	1	15.3	16.2	3.1	64.3	11.6	15.3
Zn	107	80	80	76	99	81	68	69	50	63	66	59	54	63	52	52
Y	52	49	39	43	57	63	48	48	46	47	40	39	44	41	49	48
Nb	37	31	20	22	32	37	33	34	30	32	23	26	31	30	36	31
Ba	399	479	414	310	332	355	373	413	384	361	272	323	274	322	405	443
La	70	52	30	34	43	45	50	54	51	40	27	40	42	41	53	55
Ce	128	103	58	57	66	83	79	91	98	77	45	64	74	71	96	92
Pb	37	22	10	18	18	13	21	21	15	17	10	17	18	19	21	15
Al_2O_3/TiO_2	18.98	12.87	13.61	14.23	9.53	5.02	12.45	12.13	12.09	9.86	10.26	11.12	10.23	11.54	9.93	9.01

SiO_2/Al_2O_3	1.89	2.88	3.44	2.97	3.24	4.56	3.22	3.39	3.73	4.34	5.03	4.67	4.57	4.07	4.45	4.84
Cr/Ni	2.22	2.26	2.24	1.92	1.70	1.83	2.28	2.55	2.26	2.58	2.21	2.62	3.04	1.89	3.62	2.21

Overall, it can be seen that stream sediment samples, essentially of the clay type, are the most mineralized in terms of Au, Cu, Zn and Ni, compared with sandy samples (Fig.05). In tropical environments, alteration of the mafic (basalt) to intermediate (andesite) formations of the greenstone belt will yield predominantly clay samples. Whereas in granitic formations. feldspar and ferromagnesian minerals will tend to alter into clay (kaolinite, gibbsite etc.) and the highly resistant quartz will be spared, leaving only quartz grains with clays (sandy-clay material). On the other hand, these clays are scattered and quartz grains are concentrated to form essentially sandy material. Despite all this, it is difficult to make a direct correlation between the origin of the clays and the parent rock from which they are derived. What's more, as far as metal content is concerned, there is contamination linked to artisanal gold mining. As a result, the levels of various metals in stream sediments often contrast with those in certain types of sampled material.

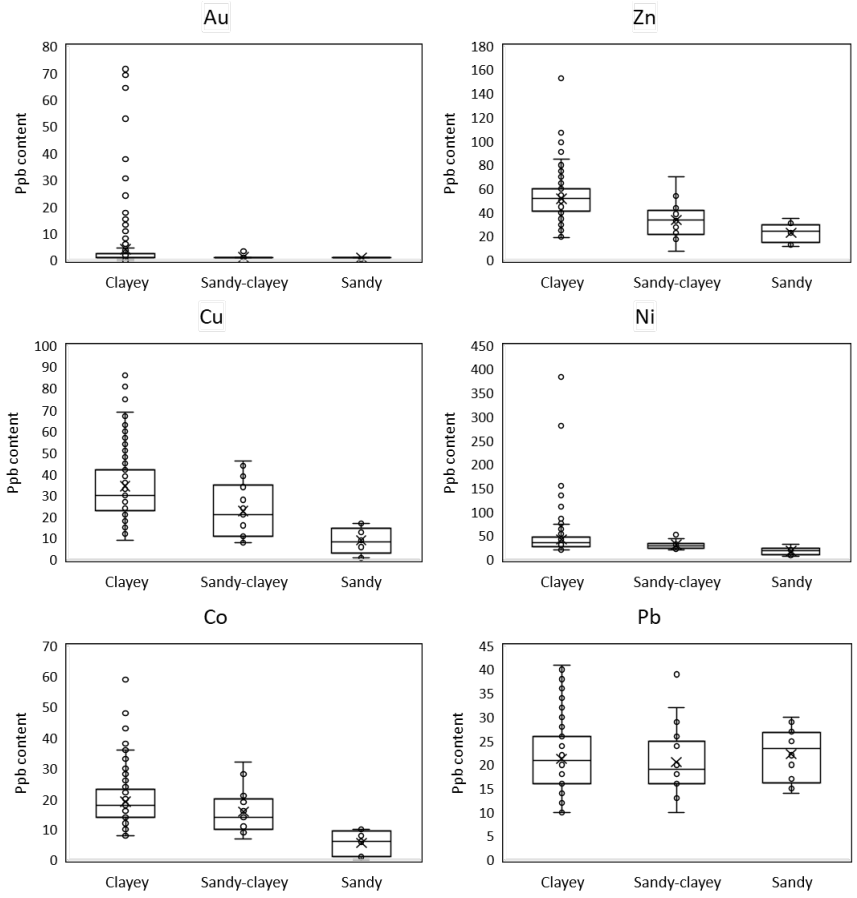

Figure 5. Moustache box plot of the distribution of various metals in stream sediments.

The spatial distribution of gold (Au) grades from total rock geochemistry shows that anomaly areas 1 and 2 are zones of high gold potential (Fig.4). Pearson correlation coefficients calculated from stream sediment data from anomaly areas 1 and 2 show an intercorrelation between certain metals (Table II). A strong correlation is observed between Ni-Cr, Cu-Co-Zn, while gold (Au) shows weaker or stronger links between Co, Cu and Zn.

Table II. Correlation matrix between metal contents from zone 1 and 2 stream sediment data (n= 53)

	Au	Co	Cr	Cu	Ni	Pb	Zn
Au	1	0.24	-0.04	0.18	-0.06	-0.15	0.08
Co		1	0.43	0.75	0.41	0.04	0.75
Cr			1	0.38	0.83	-0.11	0.32
Cu				1	0.32	-0.18	0.72
Ni					1	-0.15	0.31
Pb						1	0.25
Zn							1

Anomaly area one (01), located in the Perkoa locality, has Cu values ranging from 1.76 to 326.31 ppm, followed by Ni, Zn and Au respectively, with values up to 112 ppm (Fig.6). In zone one (01). a complex of Zn-Pb-Ag-Au anomalies has been described at the Perkoa zinc mine within the differentiated volcano-sedimentary formations of the greenstone belt (Kabore et al., 1989).

In the second anomaly area (2), Ni grades stand out with values as high as 282 ppm (Fig.7). Bouga is located within this zone, where nickel showings are reported in a Ni-Co-Cr anomaly set resulting from peridotite alteration, which extends over a small area (Kabore et al., 1989). In addition, two (02) Au-Cu-Ag anomalies have been reported in this zone at the Kwademen artisanal mine, and have been described as related to quartz veins or silicified zones mineralized with sulfide and Au (Ouedraogo, 1988).

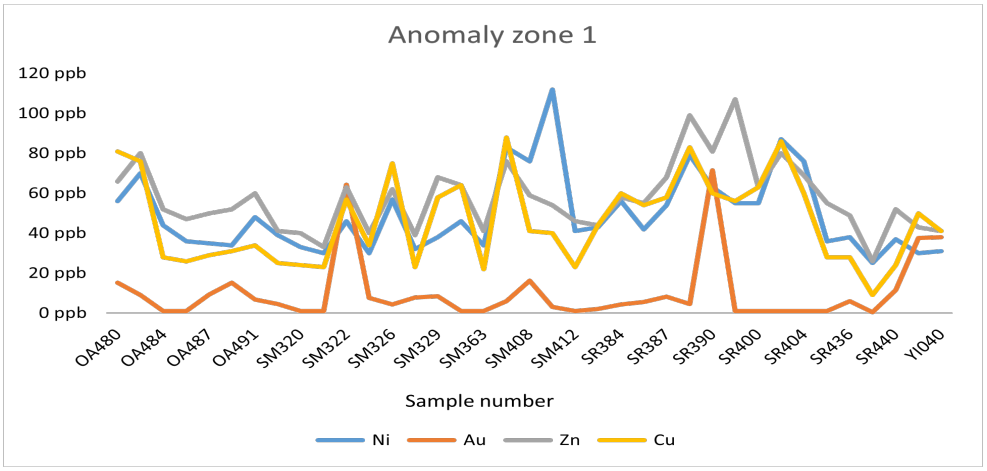

Figure 06. Au grade distribution in anomaly zone 1

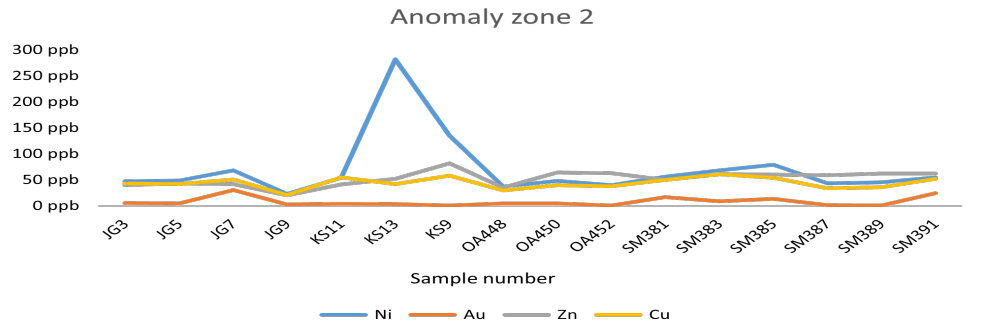

4.2 Geochemistry of volcanic units

Geochemistry on the total rock of the various volcanic units (Table III) reveals that the volcanic formations present in the study area are of basic to acidic composition, passing through the intermediate terms according to the TAS diagram (Middlemost, 1994) (Fig.8-A). These volcanic formations are essentially basalts, basaltic andesites, andesites, dacites and rhyolites. Basalt flows are characterized by variable SiO2 contents ranging from 45.09 to 50.88% (Fig.8-A). In Jensen's (1976) diagram, basalts show an affinity for the iron-rich tholeiitic series. while andesites, dacites and rhyolites are placed in the calc-alkaline series (Fig.8-B). The geodynamic environment of these basalts lies within the mid-ocean ripple field (MORB) based on the diagram of Hollocher et al., (2012) and the calc-alkaline series formations lie within the island arc field (Fig.8-C

Table III. Table of rock geochemistry data on volcanic formations

SAMPLE	E0092	MD0304	MD0321	MD0339	MD0381	MD0448	PC0297	JM0413	JM0427	JM0453	MD0340	MD034A	M
Litho	Dacite	Andesite	Andesite	Basalte	Rhyolite	Epiclastite	Basalt	Ultrabasite	Basalt	Basalt	Basalt	Basalt	
Long	-2.5	-2.5	-2.7	-2.5	-2.6	-2.8	-2.2	-2.6	-2.7	-2.6	-2.48	-2.5	
Lat	12.4	12.3	12.1	12.4	12.3	12.1	12.3	11.9	12	12	12.27	12.38	
SiO_2	69.6	60.8	55	50.5	75.1	78.2	51.3	21.7	54	50.9	49.59	49.97	
TiO_2	0.2	0.7	1.2	1.2	0	0.3	1.3	4.6	0.6	1.1	1.08	1.23	
Al_2O_3	15.3	15.8	14.7	15.2	13.8	10	17.2	61.7	13.7	14.2	14.3	15.33	
Fe_2O_3	3.1	6.4	11.5	12.9	0.6	3.1	10.4	1.3	9.6	12.7	12.68	11.84	
MnO	0.1	0.1	0.2	0.2	0.1	0.1	0.2	0	0.2	0.2	0.2	0.19	
MgO	0.7	4.2	3.8	5.5	0	0.3	5.5	0.2	3.8	4.5	6.81	6.73	
CaO	3.8	5.1	8.5	12.4	0.5	0.9	9.7	4.7	13.6	13.1	10.58	11.74	
Na_2O	5.4	3.4	3.2	1.4	4.7	2.3	2.9	0.6	1.3	1.3	1.94	2.19	
K_2O	0.6	1.8	0.3	0.2	3.8	2	0.5	1.6	0.2	0.1	0.27	0.11	
P_2O_5	0.1	0.2	0.1	0.1	<0.01	0	0.2	<0.01	0.1	0.1	0.11	0.08	
LOI	1.1	1.6	1.4	0.5	1.2	2.8	0.9	3.4	2.8	1.9	2.44	0.59	
Total	98.9	98.4	98.6	99.5	98.8	97.2	99.1	96.6	97.2	98.1	97.56	99.41	
Co	4.3	26.4	44.4	60.9	10.2	13.3	39	0	0	0	56	50.7	
Cr	139	121	3	29	6	13	10	0	0	0	40	7	
Ag	8	46	15	38	97	20	21	51	16	14	30	46	
Au	13	3	5	3	6	6	3	38	5	6	9	2	
Cu	15.9	14.6	13	97.8	3.5	3.8	28	17.1	39.2	69	106.27	154	
Mo	2.3	0.4	1.4	0.4	0.1	0.2	0.8	3.8	0.7	0.8	0.42	0.26	
Pb	0.6	10.3	3.9	3.1	54.3	11.9	3.2	9.7	17.9	21.4	11.98	3.48	
Zn	32.4	73	31	15.4	49.6	10.3	47.8	4.4	19.9	39	39.9	34.1	
Ni	9	101.4	14.4	132.2	1.1	13.6	25.3	11.7	44	55.1	143.5	109.8	
Nb	2.8	5.5	4.1	3.2	30.8	3	6.9	17.8	4.1	3.4	2.5	3.5	
Th	1.3	3.4	1.7	0.2	17.4	4.6	0.7	3.5	1.4	0.5	0.3	0.3	
La	10.6	21.4	12.6	4	6.3	28.8	11	33.6	11.4	6.7	4.5	3.8	
Ce	20.7	43	24.2	9.9	12.9	47.4	25.1	54.4	22.9	9.4	11	10.4	
Pr	2.4	5.2	3.1	1.6	1.6	5.9	3.3	7.9	3.2	2.1	1.71	1.5	
Nd	8.5	21.3	13.8	8.9	6.2	21.6	15.3	34.6	13.9	10.3	9.2	8	
Sm	1.5	4.5	3.4	2.6	1	4.1	3.2	5.1	2.8	2.9	2.7	2.5	
Eu	0.5	1.2	1	1.1	<0.5	0.9	1.4	0.5	0.9	1	0.99	1.14	
Gd	1.2	3	3.7	3.8	1	2.4	3.7	3.1	3.4	3.9	2.83	3.11	
Tb	0.2	0.5	0.7	0.6	0.2	0.3	0.6	0.5	0.6	0.7	0.54	0.5	

Dy	1	2.5	3.6	4.2	1.1	1.5	4	2.9	3.8	4.3	3.39	3.61
Ho	0.2	0.5	0.9	1	0.2	0.3	0.8	0.6	0.8	0.9	0.83	0.75
Er	0.7	1.5	2.9	2.9	1	0.9	2.4	2	2.5	2.7	2.38	2.21
Yb	0.8	1.2	2.8	2.8	1.4	0.7	2.2	2.9	2.5	2.5	2.5	2
Lu	0.1	0.2	0.4	0.4	0.2	0.1	0.4	0.5	0.4	0.4	0.32	0.31
Eu/Eu*	1.07	1.02	0.84	1.03	0.75	0.87	1.28	0.40	0.85	0.90	1.09	1.25
$(La/Yb)_N$	9.62	12.56	3.06	0.99	3.18	28.00	3.34	7.83	3.15	1.81	1.23	1.29
$(La/Sm)_N$	4.43	2.98	2.32	0.96	3.95	4.40	2.15	4.13	2.55	1.45	1.04	0.95

Rare Earth spectra normalized to the primitive mantle (McDonough and Sun, 1995) show a flat profile for basalts and this translates into low fractionation as shown by LREE/HREE ratios (La/Yb)N = 0.99 - 1.81. In contrast, the spectra of basaltic andesites, dacites and andesites show low enrichment in light rare earths (LREE). However, in the calc-alkaline series, andesite shows a high fractionation rate with sufficiently high LREE/HREE ratios (La/Yb)N = 12.56 and (La/Sm)N = 2.98 (Fig.8-D).

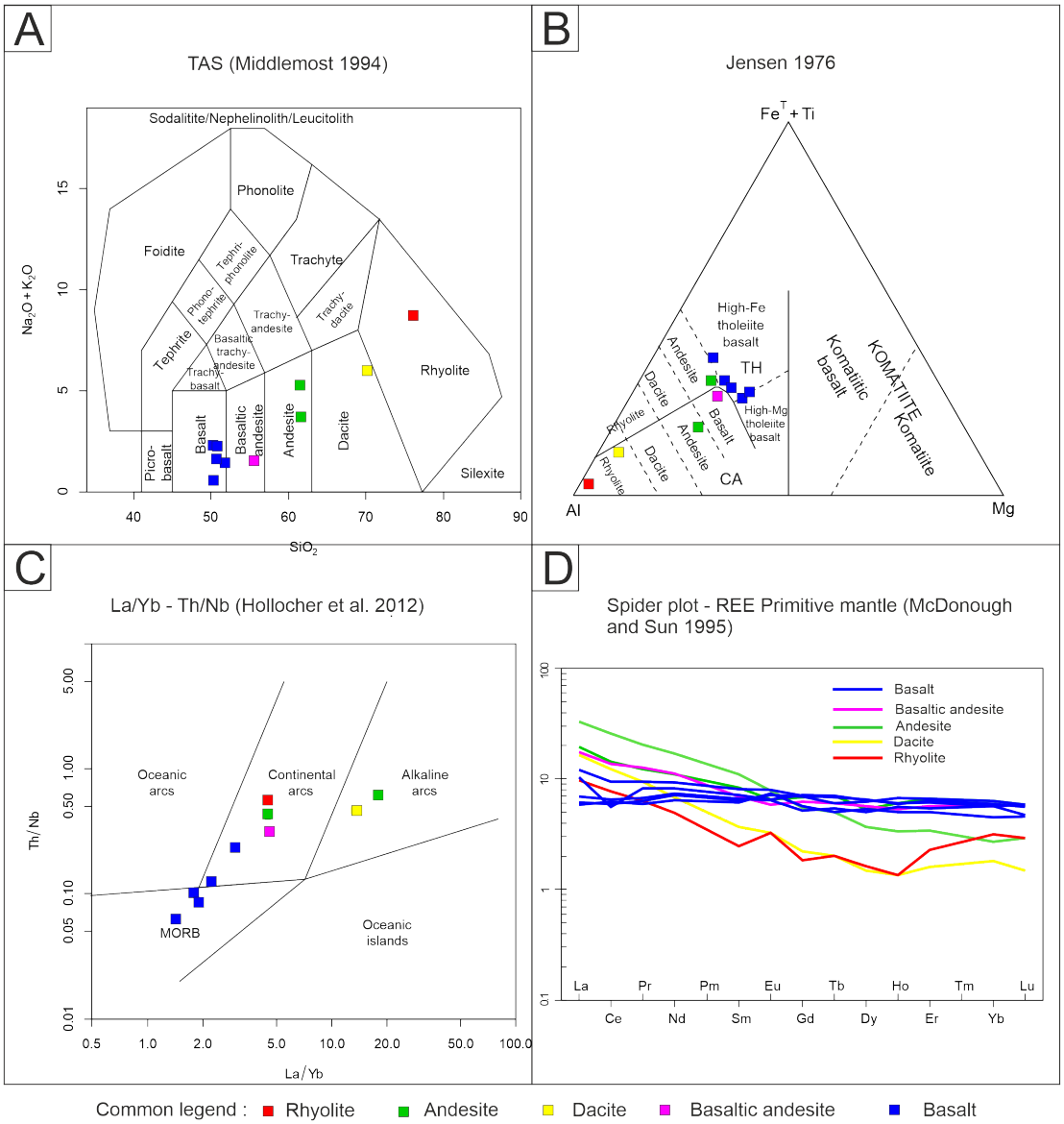

Figure 08. Geochemical characterization diagrams of volcanic formations. (A) Representation of volcanic formations in the Middlemost diagram (1994). (B) Magmatic series discrimination diagram by Jensen (1976). (C) Binary geotectonic discrimination diagram of La/Yb vs Th/Nb (Hollocher et al., 2012). (D) Rare Earth spectra of volcanic formations in the study area normalized to the Primeval Mantle (McDonough and Sun 1995)

4.3 The nature of the geochemical anomaly sets delineated

Litho-geochemistry essentially distinguishes two sets of geochemical anomalies depending on the family to which the indexed rocks belong: (i) a basic type located in the mafic to intermediate volcanic formations of the Boromo greenstone belt, and (ii) an acid type located in the granitoids with high silica (62.8 to 74.69%) and potassium (2.04 to 5.54%) contents. The basic type is relatively enriched in metals. The average gold (Au) content is 8.5 ppm in the greenstone formations, compared with an average content of 1.35 ppm in the granitoids, while the average Cu content is 36.15 ppm in the greenstone belt formations, compared with 10.1 ppm in the granitoids.Globalement. Overall, the basic type is enriched in Au, Cr, Co, Cu, Ni and Zn compared with the acidic type (Fig.9). With regard to the distribution of metal anomalies, we note that Cr and Ni are much more represented in the ultramafic volcanic formations of the belt and almost absent in granitic facies, except in contact zones with the volcanic formations of the Birimian belt and in shear zones where deformation allows mineralizing fluids to be remobilized towards these granitic formations. On the other hand, Pb is more prevalent in the granitoids, with levels ranging from 5.5 to 28.6 ppm, but is little or low in the volcanic formations of the greenstone belt.

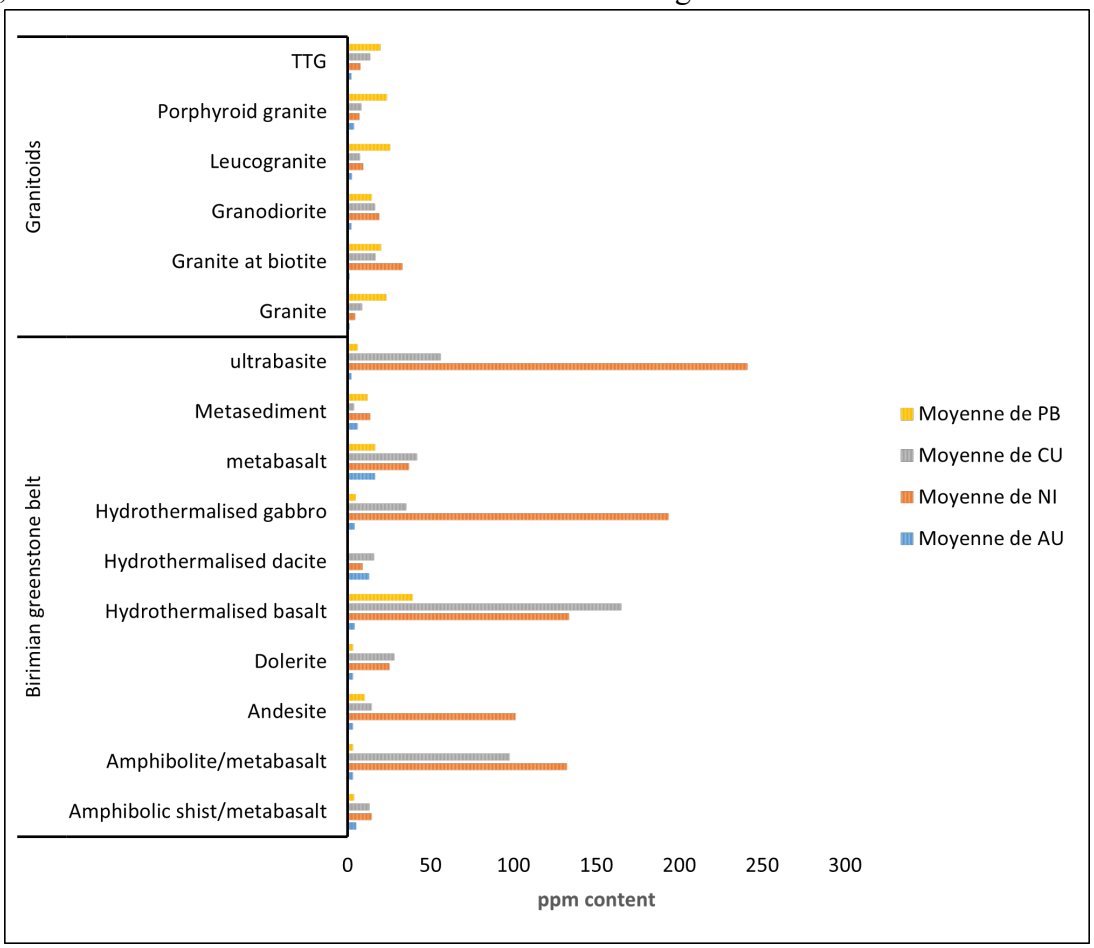

Figure 9. Histogram of average metal content in the main geological formations

5. Discussion

The Birimian formations host several gold deposits considered to be orogenic gold deposits (Milési et al., 1989, 1992 ; Groves et al., 1998; Markwitz et al., 2016; Goldfarb et al., 2017; Masurel et al., 2021). Most of these deposits are hydrothermal, i.e. linked to the circulation of fluids located in structural faults (Groves et al., 1998). They are mostly syn- to tardi-tectonic (Milési et al., 1989, 1992; François Bourges et al., 1998; Markwitz et al., 2016; Goldfarb et al., 2017; Masurel et al., 2021). Indeed, mapping and mineral exploration work in the central-western region of Burkina Faso show mostly vein-type mineralization with quartz and sulfide veins. In the discussion that follows, we will first discuss the origin of the bedrock from which the mineralized stream sediments originate, and the fertility of the formations around these sediments. We will then look at the various mineralization occurrences in the main zones.

5.1 Probable origin of stream sediments

Stream sediment data show a pronounced enrichment of Au, Cu, Ni and Zn in clay-type samples, to the detriment of sandy-type samples. The sandy-clay type is weakly mineralized in metals. This can be explained mainly by the fact that most of the samples tested in the greenstone belt formations were not only rich in gold, Cu, Ni and Zn, but also yielded clay-type sediments through supergene alteration. However, the origin of the clays is unclear, as they may originate from greenstone belt formations and/or granitoid formations. Work on granite formations shows that they weather to give sands and clays (Cullers, 1988). However, several studies have already demonstrated the importance of the granulometry of stream sediment samples for prospecting (Ndome Effoudou-Priso et al., 2014 ; Manuela Vinha G. Silva et al., 2016; Shruti et al., 2017; Sorokina, 2019). Indeed, fine fractions such as clays/limons in sediments are capable of concentrating and transporting many elements associated with most types of mineral deposits (Chandrajith et al., 2001; Manuela Vinha G. Silva et al., 2016; Martinčić et al., 1990; Melo and Fletcher, 1999; Young et al., 2013). In Sri Lanka, for example, the work of Chandrajith et al., (2001) indicates that grain size fractions below 177 ppm are considered a preferable fraction over coarse (sand) for geochemical exploration studies of stream sediments in tropical terrains with high metal gold content.

Analysis of stream sediment data for immobile major elements and trace elements such as Ti, Fe, Al, Th, Sc, Co and Zr are good indicators for tracing the source of sediments (Taylor and McLennan, 1985). Al2O3/TiO2 ratios are most often exploited to search for source rock, due to the fact that they are considered to remain constant during surface weathering (Hayashi et al., 1997; He et al., 2010; Shao et al., 2016). The Al /Ti ratio increases proportionally with Si (Hayashi et al., 1997). According to Hayashi et al. (1997), Al2O3/TiO2 ratios increase from 3 to 8, 821 and 2170 respectively in mafic, intermediate and felsic igneous source rocks. In the present study, Al2O3/TiO2 ratios range from 4 to 14 in anomaly zone one (01) for high Au samples. In anomaly zone two (02), Al2O3/TiO2 ratios also ranged from 6 to 14 for high Au grades. These results show that the origin of these gold- and metal-rich clayey sediments is predominantly from the basic to intermediate magmatic formations of the Birimian belt (Fig.10).

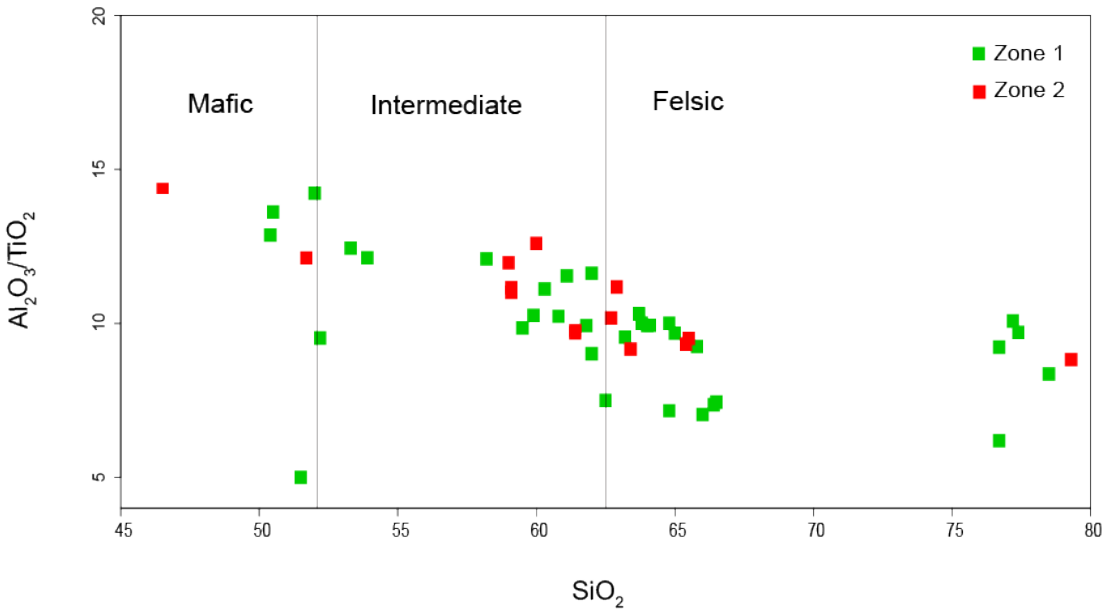

Figure 10. Binary diagram illustrating Al2O3/TiO2 vs. SiO2 ratios of stream sediments from Anomaly Zones 1 and 2. Adapted from Le Bas et al. 1986

In addition to the high gold, Cr and Ni contents in stream sediment samples, anomaly zones one (01) and two (02) delineated confirm this provenance trend. Indeed, ultrabasic rocks produce sediments with high Cr and Ni contents, while low Cr concentrations indicate a felsic origin (Wrafter and Graham, 1989; Garver et al., 1996; Armstrong-Altrin et al., 2004). Cr and Ni concentrations are particularly high in anomaly zone two (02), with Cr/Ni ratios ranging from 1.16 to 2.6 (see Table II).

5.2 Fertile gold formations

The geodynamic context of the basaltic formations of the West African Craton (WAC) is defined by two groups of authors. A first group of authors (Zonou et al., 1985; Ama Salah et al., 1996; Béziat et al., 2000; Baratoux et al., 2011; Eglinger et al., 2017; Wane et al., 2018) propose that the WAC basalts formed in a mid-ocean wrinkle context or in an island arc context. The second group of authors propose an oceanic shelf context with mantle plume activity (Abouchami et al., 1990; Boher et al.,1992; Tayllor et al., 1992; Pouclet et al., 2006, Lompo, 2009; Augustin and Gaboury, 2017). Lompo (2009) defined three types of tholeiites for the WAC formations ranging from PTH1 to PTH3.

For the geodynamic context, he proposes an oceanic basin formed by subsidence. In view of what has been said above, we propose that the basalts of the Tenado region are linked to emplacement in an oceanic plateau context in connection with mantle plume activity; as this type of basalt displays chondrite-normalized rare-earth flat spectra similar to those of the West African craton (Lompo, 2009, Augsutin and Gaboury, 2017).

This type of basalt is a primary source of gold and various metals (Augustin and Gaboury, 2017; Ouiya et al., 2022). In the same vein, earlier work by Chevremont et al., (2003) on the Koudougou square degree in the Perkoa locality showed that in the anomalies of the basaltic-type assemblage (basalt), is distinguished from other volcanic formations by its enrichment in Au, Cu and Mg (Fig. 9). This fertility of basalt in gold and other metals has also been reported in the nearby Houndé greenstone belt (Augustin and Gaboury, 2017). We showed in the previous paragraph that the gold-rich clay sediments would come from basic

5.3 Evidence of zones with high gold and base metal potential

a) Anomaly zone one (01)

This zone contains four (04) mapped gold showings in the localities of Kelsio, Zoula, Poa and Dyoro (Fig.11). In addition to these gold showings, there is the Perkoa zinc mine. The Perkoa deposit is a polymetallic Zn-Ag volcanogenic sulfide cluster (VMS) (Napon, 1988; Ouedraogo, 1989; Milési et al., 1989; Schwartz and Melcher, 2001, 2003). On the other hand, in the four (04) gold showings cited, mineralization is mainly vein-type and located in the shear zone. It takes the form of disseminated mineralization with a strong presence of sulfides in silicified zones (Ouedraogo, 1989; Kabore et al., 1989; Lompo, 1991; Chevremont et al., 2003). In these four (4) zones, gold is mined by artisanal methods (orpaillage) in quartz veinlets/veins along a N-S to NE-SW-trending structure in highly sheared metavolcanite and metasedimentary host rocks.

b) Anomaly zone two (02)

A variety of metal showings (Cu, Ni and Au) are recorded in this anomaly area. A total of five (05) showings have been recorded, covering the localities of Kwademan, Baguiomo, Bérédo, Bonga and Baganapou (Fig.12). The Bonga showing displays Ni mineralization in a zone of supergene alteration in lateritic and bauxitic formations (Kabore et al., 1989; Ouedraogo, 1989). In contrast, the Kwademen deposit shows occurrences of gold (Ouedraogo, 1989; Lompo et al., 1991) and base metals (Cu and Mn) (Lompo, 1991; Ilboudo, 2006). At Kwademen, prospecting for gold has shown that mineralization is linked to cataclasic quartz veins with free gold, gold-pyrite, arsenopyrite and chalcopyrite, mainly submeridian in orientation (Ouedraogo, 1989; Kabore et al., 1989; Lompo, 1991; Chevremont et al., 2003). The Baguiomo, Bérédo and Baganapou gold deposits occur as vein-type mineralization, with gold finely disseminated, rarely as Stockwerk in strongly hydrothermalized host rocks. Alteration in these zones varies (silicification, sericitization, etc.), but can be much more complex in faulted contact zones with granitoids. The main shear zones show similar orientations to the first anomaly area. The main gold mining activity is gold panning, but in localities such as Baguiomo, Tiekouyou and Karabole it appears to be under-explored.

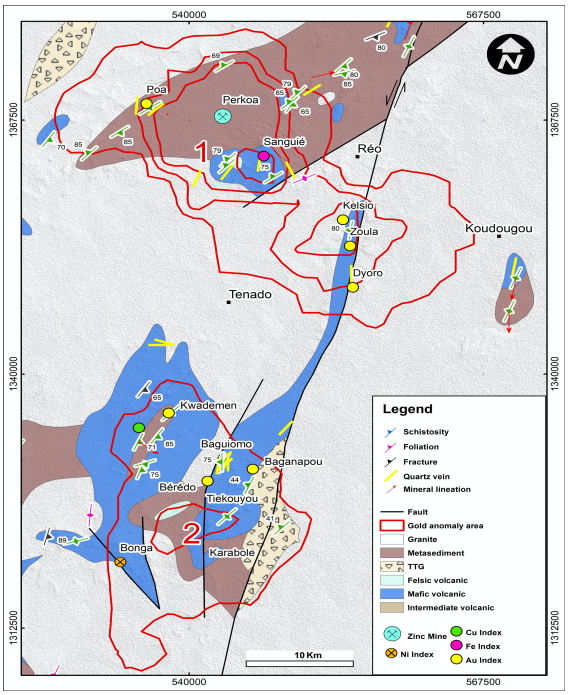

Figure 11. Structural map and mineral showings

6. Conclusion

The combination of gold content in stream sediments and litho-geochemical data has enabled us to highlight two areas of gold (Au) and miscellaneous metal anomalies. Gold content in stream sediments is mainly influenced by the parent rock from which it is derived. Stronger gold anomalies are found in clay sediments than in sandy sediments. Clay sediments are derived from basic rocks (basalt) and intermediate rocks (andesite-dacite), whereas gold-poor sandy sediments are derived from granitoids. The basic to intermediate rocks are fertile for primary gold. Anomaly zone one (01) in the northern part of the study area and anomaly zone two (02) in the southern part of the study area show occurrences of mainly gold and various metals (Zn, Cu, Ni). The evidence of these two zones thus delineated constitutes areas of major interest for gold (Au) prospecting. These zones are of greatest interest when they occur in shear zones or in close proximity to host formations affected by hydrothermal alteration. Anomaly zone two (02) is located in a shear zone.

Acknowledgements

Our first thanks go to BUMIGEB, which provided us with geochemical data for this study. The geochemical work was acquired during the SYSMIN 2003 project. This work is part of my doctoral thesis at Joseph KI-ZERBO University.

Conflit d'intérêts

Les auteurs n'ont signalé aucun conflit d'intérêts

Sample	SR385	OA505	OA491	SR436	SM329	SM363	SR406	OA484	OA485	SR382	SM412	SR384	SR438	YI036	SM324	YI040	SM30
Anomalie	Zone 1	Zone 1	Zone 1	Zone 1	Zone 1	Zone 1	Zone 1	Zone 1	Zone 1	Zone 1	Zone 1	Zone 1	Zone 1	Zone 1	Zone 1	Zone 1	Zone 1
Material	Argilaux	Argilaux	Argilaux	Argilaux	Argilaux	Argilaux	Argilaux	Argilaux	Argilaux	Sablo-argilaux	Argilaux	Argilaux	Sableux	Argilaux	Argilaux	Argilaux	Argilaux
Long	-2.52	-2.57	-2.63	-2.68	-2.52	-2.53	-2.60	-2.64	-2.63	-2.52	-2.58	-2.52	-2.69	-2.60	-2.46	-2.49	-2.52
Lat	12.35	12.45	12.39	12.41	12.29	12.19	12.25	12.33	12.36	12.36	12.43	12.37	12.41	12.37	12.21	12.25	12.29
SiO_2	62.5	63.2	63.7	63.7	63.8	64	64.1	64.8	64.8	65	65.8	66	66.4	66.5	76.7	76.7	77.2
Al_2O_3	10.8	12.8	12.7	13.8	12.4	14.3	15.5	11.1	13.1	12.2	12.3	10.7	10.3	9.3	10.8	9.6	13.7
Fe_2O_3	5.7	4.1	5	3.9	6.2	4.6	3.9	4.4	4.4	5.2	4.2	5.5	3.3	5.5	4.2	6.3	5.4
CaO																	
K_2O				1.3	0.9	0.8	1.2	0.9	1	1.1	1	0.8	1.1	0.9	1	0.7	0.9
MnO	0.11	0.05	0.08	0.05	0.12	0.06	0.18	0.17	0.04	0.09	0.1	0.09	0.07	0.06	0.07	0.07	0.1
TiO_2	1.44	1.34	1.23	1.34	1.24	1.44	1.56	1.55	1.31	1.26	1.33	1.52	1.4	1.25	1.17	1.55	1.36
Co	25	15	21	16	25	16	24	22	16	21	20	28	6	18	18	18	20
Ni	42	39	48	38	38	34	36	44	36	43	41	56	25	30	30	31	46
Cu	54	25	34	28	58	22	28	28	26	44	23	60	9	50	34	41	64
Au	5.6	4.6	6.8	6.1	8.4	1	1	1	1	2.1	1	4.3	0.5	37.7	7.7	38	1
Zn	55	41	60	49	68	41	55	52	47	44	46	58	26	43	40	41	64
Y	44	44	41	45	40	48	54	49	40	39	44	34	44	44	42	39	43
Nb	28	35	26	34	26	40	42	33	31	27	37	21	32	20	31	22	27
Ba	359	332	471	455	305	373	504	406	368	356	407	267	369	269	388	237	336
La	32	42	40	50	34	76	83	46	41	33	48	22	40	27	44	25	38
Ce	53	73	68	79	59	140	152	76	69	51	92	36	55	67	87	63	70
Pb	13	11	<10	17	13	31	27	12	11	14	21	10	16	19	20	14	10
Al_2O_3/TiO_2	7.50	9.55	10.33	10.30	10.00	9.93	9.94	7.16	10.00	9.68	9.25	7.04	7.36	7.44	9.23	6.19	10.07
SiO_2/Al_2O_3	5.79	4.94	5.02	4.62	5.15	4.48	4.14	5.84	4.95	5.33	5.35	6.17	6.45	7.15	7.10	7.99	5.64

Appendix. Table of stream sediment data for anomaly zones 1 and 2.

Cr/Ni	2.19	2.10	2.02	2.42	2.13	2.41	2.14	1.89	2.11	2.00	2.24	1.63	3.04	2.83			
Sample	SM328	SM321	KS9	KS13	SM383	SM387	SM391	KS11	OA452	SM381	SM385	OA450	SM389	JG7	JG3	JG5	OA448
Anomalie	Zone 1	Zone 1	Zone 2	Zone 2	Zone 2	Zone 2	Zone 2	Zone 2	Zone 2	Zone 2	Zone 2	Zone 2	Zone 2	Zone 2	Zone 2	Zone 2	Zone 2
Material	Argilux	Argilux	Argilux	Argilux	Argilux	Argilux	Argilux	Argilux	Argilux	Argilux	Argilux	Argilux	Argilux	Argilux	Argilux	Argilux	Argilux
Long	-2.51	-2.45	-2.66	-2.65	-2.63	-2.65	-2.67	-2.65	-2.61	-2.61	-2.64	-2.61	-2.66	-2.62	-2.55	-2.56	-2.63
Lat	12.27	12.25	11.97	11.91	12.03	12.01	12.03	11.97	12.08	12.05	12.02	12.07	12.03	11.99	11.99	11.98	12.06
SiO_2	78.5	79.9	46.6	51.7	59	59.1	59.1	60	61.1	61.4	61.4	62.7	62.9	63.4	65.4	65.5	79.3
Al_2O_3	11.2	12.6	20	16	15.8	16.3	15.2	13.6	12.6	12.4	12.6	12	17	11	11	11.7	10.5
Fe_2O_3	3.9	2.9	9.7	6.6	6.8	3.8	5.7	6	5.9	5.6	6.1	6	3.9	6.4	5.7	5.8	3.5
CaO								1.8		1.5	1.4			2.2	1.1	1.3	
K_2O	0.9	0.9	1.2	1.1	1	1.2	1.3	0.9	0.9	0.9	1	0.9	1.3	0.6	0.8	0.8	1
MnO	0.08	0.04	0.13	0.09	0.1	0.07	0.15	0.06	0.13	0.06	0.07	0.17	0.07	0.09	0.07	0.07	0.08
TiO_2	1.34	1.41	1.31	1.32	1.32	1.46	1.38	1.08	1.38	1.27	1.3	1.18	1.52	1.2	1.18	1.23	1.19
Co	16	10	31	31	23	19	33	17	27	17	21	28	20	18	13	13	16
Ni	32	30	135	282	68	43	55	54	40	56	79	48	45	68	47	49	37
Cu	23	23	58	42	61	34	52	55	38	50	54	40	36	51	43	42	30
Au	7.8	1	1	3.3	8.8	1.5	24.2	4.2	1	16.9	13.6	4.4	1	30.7	5.3	4.7	4.4
Zn	39	33	82	52	61	59	62	41	63	50	60	64	62	42	40	43	35
Y	47	50	46	46	41	52	46	33	52	38	38	42	54	30	31	32	37
Nb	38	41	26	31	27	39	29	21	33	26	25	26	41	22	26	24	30
Ba	348	323	438	387	414	502	539	356	372	345	378	379	525	220	261	295	409
La	47	54	47	53	45	69	50	29	53	33	34	37	73	21	26	26	40
Ce	99	115	72	87	59	122	86	41	97	41	48	67	127	27	36	36	67
Pb	19	17	13	12	13	22	16		26	11	12	23	22				21

Al_2O_3/TiO_2	8.36	8.94	15.27	12.12	11.97	11.16	11.01	12.59	9.13	9.76	9.69	10.17	11.18	9.17	9.32	9.51	8.82
SiO_2/Al_2O_3	7.01	6.34	2.33	3.23	3.73	3.63	3.89	4.41	4.85	4.95	4.87	5.23	3.70	5.76	5.95	5.60	7.55
Cr/Ni	1.94	2.10	1.30	1.16	2.15	2.07	1.96	2.46	1.68	2.07	2.47	1.56	2.02	2.56	2.30	2.57	1.89

References:

1. Abdolmaleki, M., Mokhtari, A.R., Akbar, S., Alipour-Asll, M., Carranza, E.J.M., 2014. Catchment basin analysis of stream sediment geochemical data: Incorporation of slope effect. Journal of Geochemical Exploration 140, 96–103. https://doi.org/10.1016/j.gexplo.2014.02.029
2. Armstrong-Altrin, J.S., Lee, Y.I., Verma, S.P., Ramasamy, S., 2004. Geochemistry of Sandstones from the Upper Miocene Kudankulam Formation, Southern India: Implications for Provenance, Weathering, and Tectonic Setting. Journal of Sedimentary Research 74, 285–297. https://doi.org/10.1306/082803740285
3. Baratoux, L., Metelka, V., Naba, S., Jessell, M.W., Grégoire, M., Ganne, J., 2011. Juvenile Paleoproterozoic crust evolution during the Eburnean orogeny (~2.2–2.0Ga), western Burkina Faso. Precambrian Research 191, 18–45. https://doi.org/10.1016/j.precamres.2011.08.010
4. Batchelor, R.A., Bowden, P., 1985. Petrogenetic interpretation of granitoid rock series using multicationic parameters. Chemical Geology 48, 43–55. https://doi.org/10.1016/0009-2541(85)90034-8
5. Bessoles, B., 1977. Géologie de l'Afrique : le craton Ouest Africain. Mém. B.R.G.M, Paris 88, 403p.
6. Béziat, D., Bourges, F., Debat, P., Lompo, M., Martin, F., Tollon, F., 2000. A Paleoproterozoic ultramafic-mafic assemblage and associated volcanic rocks of the Boromo greenstone belt: Fractionates originating from island-arc volcanic activity in the West African craton. Precambrian Research 101, 25–47. https://doi.org/10.1016/S0301-9268(99)00085-6
7. Béziat, D., Dubois, M., Debat, P., Nikiéma, S., Salvi, S., Tollon, F., 2008. Gold metallogeny in the Birimian craton of Burkina Faso (West Africa). Journal of African Earth Sciences 50, 215–233. https://doi.org/10.1016/j.jafrearsci.2007.09.017
8. Bierlein, F.P., Pisarevsky, S., 2008. PLUME-RELATED OCEANIC PLATEAUS AS A POTENTIAL SOURCE OF GOLD MINERALIZATION. Economic Geology 103, 425–430. https://doi.org/10.2113/gsecongeo.103.2.425
9. Bonhomme, M., 1962. Contribution à l'étude géochronologique de la plate-forme de l'Ouest Africain. Annals de la Faculté des Sciences de Université de ClermontFerrand Géol. Minéral 5 62.
10. Bourges, F., Debat, P., Tollon, F., Munoz, M., Ingles, J., 1998. The geology of the Taparko gold deposit, Birimian greenstone belt, Burkina Faso, West Africa, Mineralium Deposita 591–605.

11. Carranza, E.J.M., 2010. Mapping of anomalies in continuous and discrete fields of stream sediment geochemical landscapes. GEEA 10, 171–187. https://doi.org/10.1144/1467-7873/09-223
12. Castaing, C., Billa, M., Milesi, J.P., Thieblemont, D., Le Metour, J., Egal, E., Donzeau, M., Guerrot, C., Cocherie, A., Chevremont, P., Tegyey, M., Itard, Y., Zida, B., Ouedraogo, I., Kote, S., Kabore, B.E., Ouedraogo, C., Ki, J.C., Zunino, C., 2003. Notice explicative de la Carte géologique et minière du Burkina Faso à 1/1 000 000.
13. Chandrajith, R., Dissanayake, C.B., Tobschall, H.J., 2001. Application of multi-element relationships in stream sediments to mineral exploration: a case study of Walawe Ganga Basin, Sri Lanka. Applied Geochemistry 16, 339–350. https://doi.org/10.1016/S0883-2927(00)00038-X
14. Chevremont, P., Donzeau, M., Le Metour, J., Egal, E., Castaing, C., Thieblemont, D., Tegyey, M., Guerrot, C., Billa, M., Itard, Y., Delpont (BRGM), G., Ki, J.-C., Zunino (ANTEA), C., 2003. Notice explicative de la carte géologique à 1/200 000 Feuille ND-30-IV KOUDOUGOU 1ère édition, 76.
15. Cullers, R., 1988. Mineralogical and chemical changes of soil and stream sediment formed by intense weathering of the Danburg granite, Georgia, U.S.A. Lithos 21, 301–314. https://doi.org/10.1016/0024-4937(88)90035-7
16. Dahl, R., Giovenazzo, D., Hein, K.A.A., Ouédraogo, C., Séjourné, S., Ouedraogo, A., Ouédraogo, P.I., Sountra, Y., Kambou, A., Coulibaly, G.K., Nassa, O., Nassa, N., Djiguemde, S., Hema, K.A.A., Bagoro, F., Sidibé, G., 2018. Carte de synthèse géologique, structurale et des substances minérales du Burkina Faso à 1/1000000.
17. Darehshiri, A., Panji, M., Mokhtari, A.R., 2015. Identifying geochemical anomalies associated with Cu mineralization in stream sediment samples in Gharachaman area, northwest of Iran. Journal of African Earth Sciences 110, 92–99. https://doi.org/10.1016/j.jafrearsci.2015.06.009
18. De la Roche, H., Leterrier, J., Grandclaude, P., Marchal, M., 1980. A classification of volcanic and plutonic rocks using R 1 R 2 -diagram and major-element analyses — Its relationships with current nomenclature. Chemical Geology 29, 183–210. https://doi.org/10.1016/0009-2541(80)90020-0
19. Doumbia, S., Pouclet, A., Kouamelan, A., Peucat, J.J., Vidal, M., Delor, C., 1998. Petrogenesis of juvenile-type Birimian (Paleoproterozoic) granitoids in Central Côte-d'Ivoire, West Africa: geochemistry and geochronology. Precambrian Research 87, 33–63. https://doi.org/10.1016/S0301-9268(97)00201-5

20. Feybesse, J.-L., Billa, M., Guerrot, C., Duguey, E., Lescuyer, J.-L., Milesi, J.-P., Bouchot, V., 2006. The paleoproterozoic Ghanaian province: Geodynamic model and ore controls, including regional stress modeling. Precambrian Research 149, 149–196. https://doi.org/10.1016/j.precamres.2006.06.003
21. Feybesse, J.-L., Milesi, J.-P., Ouédraogo, M.F., Prost, A., 1990. La « ceinture » protérozoïque inférieure de Boromo-Goren Burkina Faso: un exemple d'interférence entre deux phases transcurrentes éburnéennes. C. R. Acad. Sci. Paris, 310 1353–1360.
22. Franceschi, G., Ouédraogo, B., 1982. Prospection minière détaillée sur l'indice Pb-Zn-Ag dans le secteur de Perkoa (NW Réo) (Rap. tech. 1 and 2), (UPV 74/004, Haute-Volta, BUVOGMIPNUD, inédit).
23. Ganne, J., Gerbault, M., Block, S., 2014. Thermo-mechanical modeling of lower crust exhumation—Constraints from the metamorphic record of the Palaeoproterozoic Eburnean orogeny, West African Craton. Precambrian Research 243, 88–109. https://doi.org/10.1016/j.precamres.2013.12.016
24. Garver, J.I., Royce, P.R., Smick, T.A., 1996. Chromium and Nickel in Shale of the Taconic Foreland: A Case Study for the Provenance of Fine-Grained Sediments with an Ultramafic Source. SEPM JSR Vol. 66. https://doi.org/10.1306/D42682C5-2B26-11D7-8648000102C1865D
25. Gasquet, D., Barbey, P., Adou, M., Paquette, J.L., 2003. Structure, Sr–Nd isotope geochemistry and zircon U–Pb geochronology of the granitoids of the Dabakala area (Côte d'Ivoire): evidence for a 2.3 Ga crustal growth event in the Palaeoproterozoic of West Africa? Precambrian Research 127, 329–354. https://doi.org/10.1016/S0301-9268(03)00209-2
26. Giovenazzo, D., Séjourné, S., Hein, K.A.A., Jébrak, M., Dahl, R., Ouedraogo, C., Ouedraogo, F.O., Wenmega, U., 2018. Notice explicative de la Carte géologique et minière du Burkina Faso á 1/1 000 000. BUMIGEB (Burkina Faso) 52.
27. Goldfarb, R.J., André-Mayer, A.-S., Jowitt, S.M., Mudd, G.M., 2017. West Africa: The World's Premier Paleoproterozoic Gold Province. Economic Geology 112, 123–143. https://doi.org/10.2113/econgeo.112.1.123
28. Groves, D.I., Goldfarb, R.J., Gebre-Mariam, M., Hagemann, S.G., Robert, F., 1998. Orogenic gold deposits: A proposed classification in the context of their crustal distribution and relationship to other gold deposit types. Ore Geology Reviews 13, 7–27. https://doi.org/10.1016/S0169-1368(97)00012-7

29. Hayashi, K.-I., Fujisawa, H., Holland, H.D., Ohmoto, H., 1997. Geochemistry of ~1.9 Ga sedimentary rocks from northeastern Labrador, Canada. Geochimica et Cosmochimica Acta 61, 4115–4137. https://doi.org/10.1016/S0016-7037(97)00214-7
30. He, Z., Xu, X., Zou, H., Wang, X., Yu, Y., 2010. Geochronology, petrogenesis and metallogeny of Piaotang granitoids in the tungsten deposit region of South China. Geochem. J. 44, 299–313. https://doi.org/10.2343/geochemj.1.0073
31. Hirdes, W., Davis, D.W., Lüdtke, G., Konan, G., 1996. Two generations of Birimian (Paleoproterozoic) volcanic belts in northeastern Côte d'Ivoire (West Africa): consequences for the 'Birimian controversy.' Precambrian Research 80, 173–191. https://doi.org/10.1016/S0301-9268(96)00011-3
32. Hollocher, K., Robinson, P., Walsh, E., Roberts, D., 2012. Geochemistry of amphibolite-facies volcanics and gabbros of the Storen Nappe in extensions west and southwest of Trondheim, western gneiss region, Norway: A key to correlations and paleotectonic settings. American Journal of Science 312, 357–416. https://doi.org/10.2475/04.2012.01
33. Ilboudo, H., 2015. A stratiform (Cu-Zn±Pb) sulphide and gold occurrences in the Kwademen Birimian system (Burkina Faso, West Africa). Asian Academic Research Journal of Multidisciplinary 2, 23p.
34. Ilboudo, H., 2006. Analyse pétrographique et métallographique des sondages carottés du prospect de Kwademen (Centre Ouest du Burkina Faso) (Mémoire de DEA). Université de Ouagadougou, Ouagadougou.
35. Irvine, T.N., Baragar, W.R.A., 1971. A Guide to the Chemical Classification of the Common Volcanic Rocks. Can. J. Earth Sci. 8, 523–548. https://doi.org/10.1139/e71-055
36. Jensen, L.S., 1976. A new cation plot for classifying subalkalic volcanic rocks. 1–21.
37. Junner, N.R., 1940. Geology of the Gold Coast and western Togoland (with revised geological map). Gold Coast Geological Survey Bulletin 11 1–40p.
38. Kabore, J., Mathez, G., Ouedraogo, M.F., Sattran, V., 1989. Prospection géochimique dans le centre et le nord-ouest du Burkina Faso. Journal of Geochemical Exploration 32, 429–435. https://doi.org/10.1016/0375-6742(89)90088-5
39. Kitson, A.E., 1918. Annual Report n°948. Gold Coast Geological Survey for 1916/17, Accra.

40. Lompo, M., 2010. Paleoproterozoic structural evolution of the Man-Leo Shield (West Africa). Key structures for vertical to transcurrent tectonics. Journal of African Earth Sciences 58, 19–36. https://doi.org/10.1016/j.jafrearsci.2010.01.005
41. Lompo, M., 1991. Etude geologique et structurale des series birimiennes de la region de kwademen-burkina faso-afrique de l'ouest.
42. Lompo, M., Caby, R., Robineau, B., 1991. Evolution structurale du Birimien au Burkina-Faso: exemple de la ceinture de Boromo–Goren dans le secteur de Kwademen (Afrique de l'Ouest). Comptes Rendus de l'Académie des Sciences de Paris Série II 313, 945–950.
43. Manuela Vinha G. Silva, M., M.S. Cabral Pinto, M., Carvalho, P.C.S., 2016. Major, trace and REE geochemistry of recent sediments from lower Catumbela River (Angola). Journal of African Earth Sciences 115, 203–217. https://doi.org/10.1016/j.jafrearsci.2015.12.014
44. Markwitz, V., Hein, K.A.A., Jessell, M.W., Miller, J., 2016. Metallogenic portfolio of the West Africa craton. Ore Geology Reviews 78, 558–563. https://doi.org/10.1016/j.oregeorev.2015.10.024
45. Martinčić, D., Kwokal, Ž., Branica, M., 1990. Distribution of zinc, lead, cadmium and copper between different size fractions of sediments II. The Krka River Estuary and the Kornati Islands (Central Adriatic Sea). Science of The Total Environment 95, 217–225. https://doi.org/10.1016/0048-9697(90)90066-4
46. Masurel, Q., Eglinger, A., Thébaud, N., Allibone, A., André-Mayer, A.-S., McFarlane, H., Miller, J., Jessell, M., Aillères, L., Vanderhaeghe, O., Salvi, S., Baratoux, L., Perrouty, S., Begg, G., Fougerouse, D., Hayman, P., Wane, O., Tshibubudze, A., Parra-Avila, L., Kouamélan, A., Amponsah, P.O., 2021. Paleoproterozoic gold events in the southern West African Craton: review and synopsis. Miner Deposita. https://doi.org/10.1007/s00126-021-01052-5
47. McDonough, W.F., Sun, S. -s., 1995. The composition of the Earth. Chemical Geology 120, 223–253. https://doi.org/10.1016/0009-2541(94)00140-4
48. Melo, G., Fletcher, W.K., 1999. Dispersion of gold and associated elements in stream sediments under semi-arid conditions, northeast Brazil. Journal of Geochemical Exploration 67, 235–243. https://doi.org/10.1016/S0375-6742(99)00053-9
49. Metelka, V., Baratoux, L., Naba, S., Jessell, M.W., 2011. A geophysically constrained litho-structural analysis of the Eburnean

greenstone belts and associated granitoid domains, Burkina Faso, West Africa. Precambrian Research 190, 48–69. https://doi.org/10.1016/j.precamres.2011.08.002
50. Middlemost, E.A.K., 1994a. Naming materials in the magma/igneous rock system. Earth-Science Reviews 37, 215–224. https://doi.org/10.1016/0012-8252(94)90029-9
51. Middlemost, E.A.K., 1994b. Naming materials in the magma/igneous rock system. Earth-Science Reviews 37, 215–224. https://doi.org/10.1016/0012-8252(94)90029-9
52. Milési, J.-P., Feybesse, J.-L., Ledru, P., Dommaget, A., Ouédraogo, M.F., Marcoux, E., Prost, A., Vinchon, C., Sylvain, J.-P., Johan, V., Tegyey, M., Calvez, J.-Y., Lagny, P., 1989. Les minéralisations aurifères de l'Afrique de l'Ouest. Chronique Recherche Minière, n°497 3–98.
53. Milési, J.-P., Ledru, P., Feybesse, J.-L., Dommanget, A., Marcoux, E., 1992. Early Proterozoic ore deposits and tectonics of the Birimian orogenic belt, West Africa. Precambrian Research - PRECAMBRIAN RES 58, 305–344. https://doi.org/10.1016/0301-9268(92)90123-6
54. Miyashiro, A., 1974. Volcanic rock series in island arcs and active continental margins. American Journal of Science 274, 321–355. https://doi.org/10.2475/ajs.274.4.321
55. Napon, S., 1988. Le gisement d'amas sulfuré (Zn-Ag) de Perkoa dans la Povince du Sangyé (Burkina Faso,Afrique de l'Ouest) : Cartographie, Etude pétrographique, géochimique et métallogénique. Thèse Doc. Univ. Franche-Comté, France 309.
56. Ndome Effoudou-Priso, E., Onana, V.L., Boubakar, L., Beyala, V.K.K., Ekodeck, G.E., 2014. Relationships between major and trace elements during weathering processes in a sedimentary context: Implications for the nature of source rocks in Douala, Littoral Cameroon. Geochemistry 74, 765–781. https://doi.org/10.1016/j.chemer.2014.05.003
57. Noa Tang, S.D., Ntsama Atangana, J., Onana, V.L., 2020. Mineralogy and geochemistry of alluvial sediments from the Kadey plain, eastern Cameroon: Implications for provenance, weathering, and tectonic setting. Journal of African Earth Sciences 163, 103763. https://doi.org/10.1016/j.jafrearsci.2020.103763
58. Ouedraogo, F.O., 1988. The Kwademen Gold Deposit : a polymorphic mineralization within a Precambrian (Birrimian) greenstone belt in Burkina Faso, West Africa: a Case History. AusIMM, Perth, Symposia Series.

59. Ouedraogo, M.F., 1989. Eléments de synthèse sur l'évolution géostructurale et la métallogénie de la ceinture birrimienne de Boromo (Protérozoïque inférieur, Burkina Faso). Thèse Doct. Sci., Univ. Orléans, France 115p.
60. Peccerillo, A., Taylor, S.R., 1976. Geochemistry of eocene calc-alkaline volcanic rocks from the Kastamonu area, Northern Turkey. Contr. Mineral. and Petrol. 58, 63–81. https://doi.org/10.1007/BF00384745
61. Schwartz, M.O., Melcher, F., 2003. The Perkoa Zinc Deposit, Burkina Faso. Economic Geology 98, 1463–1485. https://doi.org/10.2113/gsecongeo.98.7.1463
62. Schwartz, M.O., Melcher, F., 2001. The geology of the Perkoa zinc deposit, Burkina Faso. Workshop VMS potential in the Birimian. BGR/BUMIGEB, Ouagadougou.
63. Shao, L., Cao, L., Pang, X., Jiang, T., Qiao, P., Zhao, M., 2016. Detrital zircon provenance of the Paleogene syn-rift sediments in the northern South China Sea: PALEOGENE SOURCE OF NORTHERN SOUTH CHINA SEA. Geochem. Geophys. Geosyst. 17, 255–269. https://doi.org/10.1002/2015GC006113
64. Shine, Y.J., Moye, C.D., Mallya, G.J., Tamambele, A.L., 2022. Generation of Geochemical Exploration Targets from Regional Stream Sediment Data Using Principal Component and Factor Ana. Tanz. J. Sci. 48, 668–679. https://doi.org/10.4314/tjs.v48i3.14
65. Shruti, V.C., Jonathan, M.P., Rodríguez-Espinosa, P.F., Nagarajan, R., Escobedo-Urias, D.C., Morales-García, S.S., Martínez-Tavera, E., 2017. Geochemical characteristics of stream sediments from an urban-volcanic zone, Central Mexico: Natural and man-made inputs. Geochemistry 77, 303–321. https://doi.org/10.1016/j.chemer.2017.04.005
66. Sorokina, O.A., 2019. Reconstruction of Sources in River Sediments in the Lower Part of the Bureya River Based on Geochemical Indices. Russian Journal of Pacific Geology 13, 176–185. https://doi.org/10.1134/S1819714019020088
67. Taylor, S.R., McLennan, S.M., 1985. The Continental Crust: Its Composition and Evolution. Blackwell Scientific Publications 312.
68. Webber, A.P., Roberts, S., Taylor, R.N., Pitcairn, I.K., 2013. Golden plumes: Substantial gold enrichment of oceanic crust during ridge-plume interaction. Geology 41, 87–90. https://doi.org/10.1130/G33301.1
69. Wrafter, J.P., Graham, J.R., 1989. Short Paper: Ophiolitic detritus in the Ordovician sediments of South Mayo, Ireland. JGS 146, 213–215. https://doi.org/10.1144/gsjgs.146.2.0213

70. Young, S.M., Pitawala, A., Ishiga, H., 2013. Geochemical characteristics of stream sediments, sediment fractions, soils, and basement rocks from the Mahaweli River and its catchment, Sri Lanka. Geochemistry 73, 357–371. https://doi.org/10.1016/j.chemer.2012.09.003
71. Yousefi, M., Carranza, E.J.M., Kamkar-Rouhani, A., 2013. Weighted drainage catchment basin mapping of geochemical anomalies using stream sediment data for mineral potential modeling. Journal of Geochemical Exploration 128, 88–96. https://doi.org/10.1016/j.gexplo.2013.01.013